Current Opinion in Solid State & Materials Science 24 (2020) 100808

Contents lists available at ScienceDirect

Current Opinion in Solid State & Materials Science

journal homepage: www.elsevier.com/locate/cossms

On Distribution of Superconductivity in Metal Hydrides

Dmitrii V. Semenok[a,*], Ivan A. Kruglov[b,c], Igor A. Savkin[d], Alexander G. Kvashnin[a,b,*], Artem R. Oganov[a,b,e]

[a] Skolkovo Institute of Science and Technology, Skolkovo Innovation Center, 3 Nobel Street, Moscow 121205, Russia
[b] Moscow Institute of Physics and Technology, 9 Institutsky Lane, Dolgoprudny 141700, Russia
[c] Dukhov Research Institute of Automatics (VNIIA), Moscow 127055, Russia
[d] Research Computer Center of Lomonosov Moscow State University, Moscow, Russia
[e] International Center for Materials Discovery, Northwestern Polytechnical University, Xi'an 710072, China

ARTICLE INFO

Dedicated to the 150th anniversary of Mendeleev's Periodic Law.

Keywords:
USPEX, High-pressure
Superconducting hydrides
Periodic Table
DFT
Evolutionary algorithm
Neural network

ABSTRACT

Using the data on the superconducting critical temperature (T_C) for a number of metal hydrides, we found a rule that makes it possible to predict the maximum T_C based only on the information about the electronic structure of metal atoms. Using this guiding principle, we explored the hydride systems for which no reliable information existed, predicted new higher hydrides in the K-H, Zr-H, Hf-H, Ti-H, Mg-H, Sr-H, Ba-H, Cs-H, and Rb-H systems at high pressures, and calculated their T_C. The highest-temperature superconducting hydrides are formed by metals in the "lability belt" roughly between 2nd and 3rd groups of the Periodic Table. Results of the study of actinoids and lanthanoids show that they form highly symmetric superhydrides XH_7-XH_9, but the increasing number of d- and especially f-electrons affects superconducitivity adversely. Hydrides of late transition metals (e.g. platinoids) and all but early lanthanoids and actinoids are not promising for high-Tc superconductivity. Designed neural network allowing the prediction of T_C of various hydrides shows high accuracy and was used to estimate upper limit for T_C of hydrides for which no date are avilable. The developed rule, based on regular behavior of the maximum achievable critical temperature as a function of number of $d + f$ electrons, enables targeted predictions about the existence of new high-T_C superconductors.

1. Introduction

Recent progress in experimental synthesis and measurement of superconducting properties of H_3S [1], H_3Se [2,3], Si_2H_6 [4], LaH_{10} [5–7], FeH_5 [8,9], UH_7 [10], CeH_9 [11,12], ThH_9 and ThH_{10} [13], PrH_9 [14], and NdH_9 [15] together with theoretical predictions including the above compounds and LiH_8 [16], CaH_6 [17], BaH_6 [2], TaH_6 [29], ScH_9 [20], VH_8 [21], SrH_{10} [18], YH_{10} [22], LaH_{10} [22], ThH_{10} [23], and AcH_{10} [24], emphasizes the need for a law governing the distribution of superconducting properties of metal hydrides over Mendeleev's Periodic Table. We have suggested earlier [24] that the majority of high-T_C metal hydrides are formed by metals at the border between *s/p* and *s/d* blocks, i.e. between the 2nd and 3rd groups; we call this region the "lability belt". The possible reason [24] is the anomalously strong electron-phonon interaction due to small energy difference between the *s*- and *-p* or *d*-orbitals of metals atoms under pressure.

Here, using this idea of "orbital lability" (i.e. the particular sensitivity of orbital populations to the environment for atoms of the elements in the "lability belt") we predict new superconducting hydrides that have not been studied yet. We considered the maximum value of T_C achieved among all stable compounds in each M−H system at all pressures found in literature as a target value for this study, i.e. $F = \max T_C(P, M_nH_m)$. To describe the behavior of F as a function of pressure P, hydrogen content N_H, and the total number of *d*- and *f*-electrons N_{d+f}, we analyzed the maxT_C-N_{d+f}, maxT_C-P, and maxT_C-N_H diagrams. Those systems for which we could not find reliable data on stable polyhydrides and their T_C were carefully investigated.

2. Methods

A powerful tool for predicting thermodynamically stable compounds at given pressure, the evolutionary algorithm USPEX [25–27], was used to perform variable-composition searches of the M_xH_y phases (M = K, Ca, Zr, Hf, Pr, Nd, Ho, Er, Tm, Lu, Pa, Np, Am, Cm) at pressures of 50, 150, 250, and 300 GPa. The first generation of 120 structures was created using random symmetric and random topological [28] generators, while all subsequent generations contained 20% of random structures and 80% of structures created using heredity, softmutation,

* Corresponding authors at: Skolkovo Institute of Science and Technology, Skolkovo Innovation Center, 3 Nobel Street, Moscow 121205, Russia (A.G. Kvashnin).
E-mail addresses: dmitrii.semenok@skoltech.ru (D.V. Semenok), A.Kvashnin@skoltech.ru (A.G. Kvashnin).

https://doi.org/10.1016/j.cossms.2020.100808
Received 16 October 2019; Received in revised form 8 February 2020; Accepted 10 February 2020
Available online 07 April 2020

and transmutation operators. The evolutionary searches were combined with structure relaxations using density functional theory (DFT) [29,30] within the generalized gradient approximation (the Perdew-Burke-Ernzerhof functional) [31] and the projector augmented wave method [32,33] as implemented in the VASP code [34–36]. The plane wave kinetic energy cutoff was set to 600 eV and the Brillouin zone was sampled using the Γ-centered *k*-points meshes with the resolution of $2\pi \times 0.05$ Å^{-1}.

Phonon frequencies and electron–phonon coupling (EPC) coefficients were computed using density-functional perturbation theory [37], employing the plane-wave pseudopotential method with the norm-conserving Troullier-Martins pseudopotentials and the Perdew-Burke-Ernzerhof exchange-correlation functional [31] as implemented in QUANTUM ESPRESSO (QE) package [38]. The $3s^23p^64s^1$, $3s^23p^64s^2$, $3d^24s^2$, $4d^25s^2$, $4f^{14}5d^26s^2$, $6s^24f^3$, $6s^24f^4$, $6s^24f^{11}$, $6s^24f^{12}$, $6s^24f^{13}$, $6s^24f^{14}5d^1$, $7s^26d^15f^2$, $7s^26d^15f^4$, $7s^15f^7$, $7s^26d^15f^7$ electrons of K, Ca, Zr, Hf, Pr, Nd, Ho, Er, Tm, Lu, Pa, Np, Am, Cm were treated explicitly. Convergence tests showed that for all elements 120 Ry is a suitable kinetic energy cutoff for the plane wave basis set. In our *ab initio* calculations of the electron–phonon coupling parameter λ, the first Brillouin zone was sampled using 2 × 2 × 2 or 4 × 4 × 4 *q*-points meshes and denser 16 × 16 × 16 and 24 × 24 × 24 *k*-points meshes. The superconducting transition temperature T_C was estimated using the Allen-Dynes formula with $\mu^* = 0.1$ (see Supporting Information for details).

A regression model was created on the basis of a fully connected (each next layer is connected with all outputs of the previous one) neural network to predict maxT_C = Y(A,B) for ternary systems A-B-H where data were lacking. It was found empirically that the optimal topology consists of 11 layers of 12 neurons in a layer. The number of *s*-, *p*-, *d*-, and *f*-electrons in an atom and the atomic number were used as input for this network. The neural network was trained on a set of 180 reference maxT_C values of binary (A-A-H, A-H-H) and ternary hydrides using the RMSProp (Root Mean Square Propagation) method in 50,000 steps. Boundary (Y(A,1) = Y(1,A) = Y(A,A)) and symmetry (Y(A,B) = Y(B,A)) conditions were included in the training set. The *tensorflow* library was applied to create the model. After the training, the network was validated on 20% randomly selected maxT_C points. The average error for binary systems did not exceed 20 K.

3. Results and discussion

3.1. Period 4. K–Ca–Sc–Ti–V–Cr

The main results for period 4 of Mendeleev's Periodic Table are presented in Table 1 and Fig. 1. The highest T_C reaches 235 K for CaH_6 [17]. The highest-T_C potassium hydride is *C*2/*c*-KH_6 with the maximum T_C of 70 K at 166 GPa, predicted by Zhou et al. [39] (Table 1). We expect that an increase in the number of *d*-electrons in the Sc-Ti-V-Cr row should lead to a smooth drop in T_C: maxT_C(Sc-H) > maxT_C(Ti-H) > maxT_C(V-H) > maxT_C(Cr-H). Since no reliable data on titanium polyhydrides were available below 250 GPa (Table 1), except TiH_2 having a low T_C = 6.7 K, we decided to perform additional computational searches for new polyhydrides in the K-H, Ca-H, and Ti-H systems.

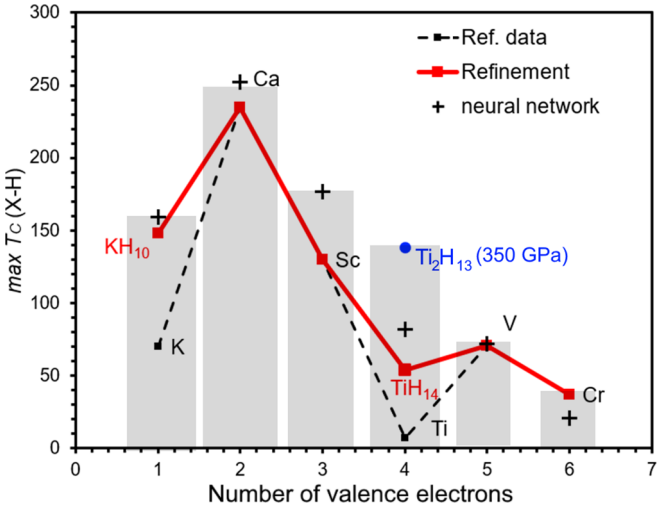

Fig. 1. Maximum T_C of hydrides of metals from 4th period.

Because the 3*d*-shell of the considered row of metals begins to be filled with electrons starting from Sc, we presumed that the energy difference between the *s*- and *d*-orbitals will decrease as pressure increases. By analogy with *d*-elements, higher hydrides of potassium and calcium, KH_n and CaH_n, with n > 6 (e.g. n = 10, 12 …), may also be formed. To test this idea, we performed variable-composition evolutionary searches for stable hydrides in the K-H and Ca-H systems at various pressures. The predicted thermodynamically stable compounds are shown in Table 2 and Table 3. The convex hull for the K-H system at 150 GPa is shown in Fig. 2, while the convex hull at 50 GPa and those for the Ca-H system are shown in Supporting Information Figs. S1 and S2, respectively.

In the K-H system we predicted new thermodynamically stable polyhydrides which have not been considered before [2,43]. We found that *Cmcm*-KH_5 [44] removes previously predicted *C*2/*c*-KH_6 from the convex hull at 150 GPa (Fig. 2). KH_5 as well as the predicted *Imm*2-KH_{11} are semiconductors with DFT band gaps of ~1 eV and 2.03 eV at 100 and 50 GPa, respectively (the systematic underestimation of the band gap by the DFT-PBE method should be taken into account). Superconducting properties were studied only for the metallic *Immm*-KH_{10} and *Immm*-KH_{12}. The newly predicted *Immm*-KH_{10} displays the highest T_C = 148 K among all the K-H phases (Supporting Information Fig. S1), while for *Immm*-KH_{12} T_C is 116 K.

The comparison of our results with the data from Refs. [15,41] points to potential existence of new stable calcium superhydrides, *C*2/

Table 1
Previously predicted or synthesized binary hydrides with maximum T_C, period 4.

Hydride (pressure, GPa)	λ	ω_{log}, K	maxT_C, K
KH_6 (166)	0.9	1165	70 [39]
CaH_6 (150)	2.7	–	235 [17]
ScH_9 (300)	1.94	1156	163 [20,40]
TiH_2 (0)	0.84	127	6.7 [41]
VH_8 (200)	1.13	876	71.4 [21]
CrH_3 (81)	0.95	568	37.1 [42]
Newly predicted compounds			
KH_{10} (150)	1.34	1301	148
TiH_{14} (200)	0.81	1063	54

Table 2
Predicted stable phases in the K-H system at 50 and 150 GPa.

Pressure, GPa	Stable phases
50	*Imm*2-KH_{11} *Pm-3m*-KH *Cm*-KH_9 *Cmcm*-KH_5
150	*Immm*-KH_{10} *Immm*-KH_{12} *Pm-3m*-KH *Cmcm*-KH_5 *C*2/*m*-KH_2

Table 3
Predicted stable phases in the Ca-H system at 0-200 GPa.

Pressure, GPa	Stable phases	Pressure, GPa	Stable phases
0	*Pnma*-CaH_2	150	*Im*$\bar{3}$*m*-CaH_6
50	*I4/mmm*-CaH_4		*P1*-CaH_6
	P6$_3$*/mmc*-CaH_2		*C2*-CaH_{18}
	R$\bar{3}$*c*-Ca_3H		*C2/m*-CaH_{12}
	I$\bar{4}$3*d*-Ca_3H_4		*I4/mmm*-CaH_4
			P6$_3$*/mmc*-CaH_2
			C2/m-Ca_2H
			Pm-CaH
100	*Pm*-CaH_2	200	*C2*-CaH_{18}
	I4/mmm-CaH_4		*Im*$\bar{3}$*m*-CaH_6
	C2/m-CaH_8		*Cmcm*-CaH_4
	P$\bar{1}$-CaH_{14}		*Imma*-CaH_2
	I$\bar{4}$3*d*-Ca_3H_4		*P6/mmm*-CaH_2
	P$\bar{1}$-$Ca_{12}H$		*Pm*$\bar{3}$*m*-CaH

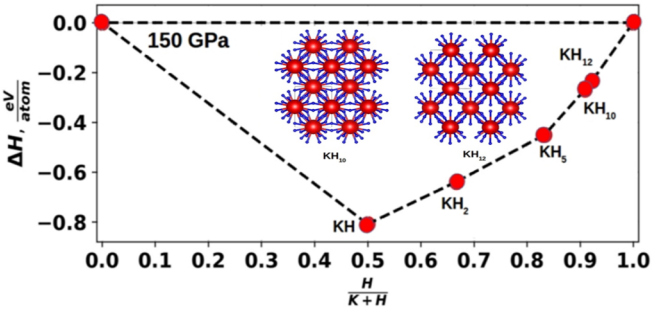

Fig. 2. Convex hull for the K-H system at 150 GPa.

m-CaH_{12} and *C2*-CaH_{18}, which were predicted at pressures up to 200 GPa (Table 3). *C2/m*-CaH_{12} has T_C = 206 K and a high EPC coefficient λ = 2.16 (Supporting Information Fig. S2), while molecular *C2*-CaH_{18} has a lower T_C = 88 K at 150 GPa. These predicted phases have a lower T_C than that of *Im*$\bar{3}$*m*-CaH_6 [17]. Using *ab initio* simulations Shao et al. [46] recently found even higher T_C for *C2/m*-CaH_9 – up to 285 K at 400 GPa.

In the Ti-H system, we predicted one new higher hydride, *C2/m*-TiH_{14}, which is thermodynamically stable at 200 GPa (Supporting Information Table S1). This hydride features superconductivity with T_C = 54.2 K (Supporting Information Fig. S23). More detailed study of Ti-H system done by Zhang et al. [47] showed existence of surprising phases *Immm*-Ti_2H_{13} and *C2/m*-TiH_{22}, which demonstrate even better superconducting properties: T_C up to 149 and 110 K at 350 and 250 GPa, respectively. These additional data eliminate the abrupt minimum at N_d = 4, making the max$T_C(N_d)$ function decrease more monotonically from Ca to Cr (red dotted line and gray columns in Fig. 1).

Thus, additional variable-composition evolutionary searches for stable phases in the K-H, Ca-H, and Ti-H systems reveal the existence of new polyhydrides with T_C exceeding the values known to date, supporting our rule of maximum T_C for electronically labile "boundary" elements, at the boundary between s|d and s|p blocks.

3.2. Period 5. Rb–Sr–Y–Zr–Nb–Mo–Tc

Some of the metal hydrides from period 5 have been studied earlier [17,43,44,16,20] (Table 4). However, no reliable information is available about the superconducting properties of the Mo-H compounds. Hooper et al. [50] studied the Rb-H system (RbH_9-RbH_{14}) only at 250 GPa, but superconductivity was not investigated. Machine learning (ML) approach [51], validated by AIRSS calculations, led to prediction of *C2/m*-RbH_{12} with T_C up to 133 K at 150 GPa, which is higher than our ML results (75 K, Fig. S30).

At 300 GPa, the *Cmca*-SrH_{10} [18], constructed on the basis of

Table 4
Predicted or synthesized binary hydrides and their maximum critical temperatures, period 5.

Hydride (Pressure, GPa)	λ	ω_{log}, K	maxT_C, K
SrH_{10} (300)	3.08	767	259 [18]
YH_{10} (300)	2.6	1282	323 [22]
ZrH (120)	0.71	295	10 [49]
ZrH_6 (295)	1.7	914	153 [53]
ZrH_{10} (250)	1.77	1068	198 [55]
NbH_4 (300)	0.82	938	38 [19]
TcH_2 (200)	0.52	736	11 [48]
Newly predicted compounds			
ZrH_{16} (200)	1.19	852	88
SrH_6 (100)	1.65	1316	189

rhombohedral structure of molecular hydrogen, is predicted to have high T_C = 259 K and large λ = 3.08, indicating the possibility to find high-T_C superconductors in the Sr-H system. Our USPEX search at 50, 100, and 150 GPa (Supporting Information Figs. S3 and S4) showed the presence of many stable and metastable higher strontium polyhydrides. At 50 GPa *I4/mmm*-SrH_4 is stable, isostructural to the previously found CaH_4 [45,52]. However, there are many low-symmetry higher hydrides in close proximity to the convex hull. At 100 and 150 GPa, *R*$\bar{3}$*m*-SrH_6 and molecular *C2/m*-SrH_{10} are found to be stable and located on the convex hull (see Fig. S28 for superconducting properties). SrH_6 becomes stable at 100 GPa, i.e. at much lower pressure than its analog *Im*$\bar{3}$*m*-CaH_6 [17] (200 GPa). These two compounds possess remarkable superconducting properties, and at 200 GPa T_C of *R*$\bar{3}$*m*-SrH_6 may exceed 189 K (Supporting Information Fig. S29). In our calculations from 50 to 300 GPa we could not find any stable high-symmetry phases of SrH_{10}.

The values of maxT_C for the rest of the metal hydrides from period 5 drop from 323 K for YH_{10} at 250 GPa [22], to 11 K for TcH_2 studied at 200 GPa [48] (Fig. 3). The maxT_C function suffers a suspicious drop at Zr, because the only known stable compound in the Zr-H system is ZrH displaying a low T_C of 10 K. In Ref. [53], novel *P2*$_1$*/c*-ZrH_6 having T_C = 153 K at 295 GPa was predicted using the random structure search (green point in Fig. 3). Taking into account a low number of valence *d*-electrons, we undertook a variable-composition evolutionary search for new stable zirconium hydrides and studied in detail the superconducting properties. At various pressures, we predicted new higher hydrides, differing from the prediction made in Ref. [53]

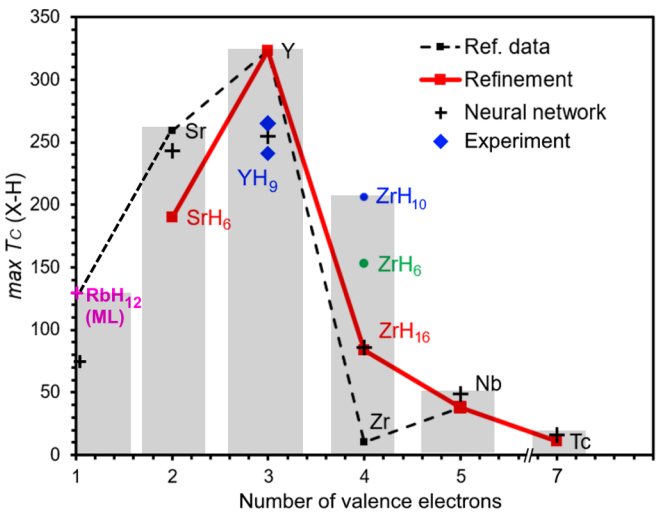

Fig. 3. Maximum T_C of hydrides of metals from 5th period. Current experimental data of T_C for YH_9 were taken from Refs. [56,57].

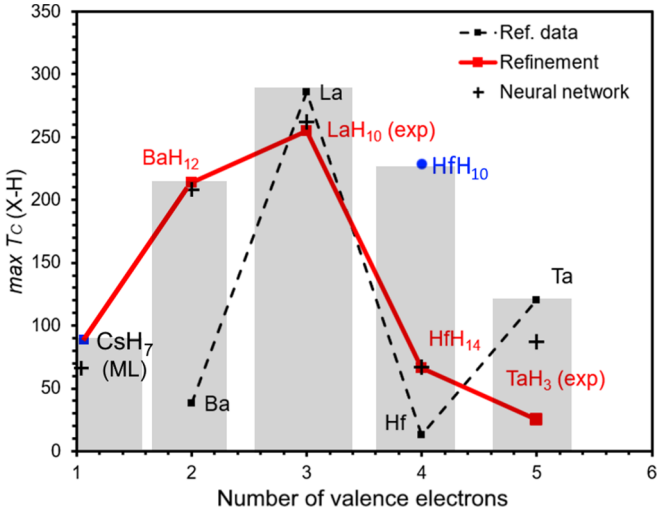

Fig. 4. Maximum T_C of hydrides of metals from 6th period. For LaH_{10} and TaH_3, the recent experimental results from Refs. [6,7,61] are presented. *hcp*-HfH_{10} was taken from Ref. [55].

(Supporting Information Fig. S5 and Table S2). The newly predicted molecular $P\bar{1}$-ZrH_{16}, stable at the pressures over 150 GPa, is the most promising among all stable phases because of the high hydrogen concentration (Table S2), having a structure close to that of titanium hydride $P2_1/c$-TiH_{14}. The calculated value of T_C of $P\bar{1}$-ZrH_{16} is 88 K. With the new ZrH_{16}, the maxT_C function for period 5 becomes much more regular (red solid line in Fig. 3), consistent with the general idea of decreasing of maximum T_C with the growing number of outer electrons in metal atoms. Recent experimental [54] and theoretical [55] studies indicate the existence of cubic ZrH_3 and Zr_4H_{15} with T_C (exp) < 7 K, and $P6_3/mmc$-ZrH_{10} with $\lambda = 1.77$ and T_C(theory) up to 198 K at 250 GPa, which also agrees with our proposed dependence of maxT_C(N_d). It should be noted that predicted in Ref. [55] $P6_3/mmc$-ZrH_{10} is thermodynamically stable and changes the convex hull at 250 GPa (Fig. S5).

3.3. Period 6. Cs–Ba–La–Hf–Ta

Available data on superconducting properties of the predicted or synthesized metal hydrides from period 6 of Mendeleev's Table are shown in Fig. 4 and Table 5. Shamp et al. [58] predicted several Cs-H compounds, namely CsH_7 and CsH_{16}, presumably stable at 150 GPa, but their superconducting properties were not studied. Machine learning approach [51], validated by AIRSS calculations, led to prediction of possible low symmetry CsH_7 with T_C up to 90 K at 100 GPa, which is close to our neural network (ML) results (65 K, Fig. S30). In the Ba-H system, BaH_6 displays the maximum value of T_C = 31–38 K at 100 GPa [2], whereas LaH_{10} displays T_C = 286 K at 210 GPa [22]. In the Hf-H system, only HfH_2 is known with T_C of 13 K at 260 GPa [59] (Fig. 4). In the Ta-H system, *Fdd2*-TaH_6 was predicted to have T_C = 136 K at 300 GPa [60]. A sharp drop in maxT_C at Hf (Fig. 4), similar to Zr (Fig. 3), indicates the lack of data about the possible superconducting polyhydrides in the Hf-H system.

Table 5
Predicted binary hydrides and their maximum critical temperatures, period 6.

Hydride (Pressure, GPa)	λ	ω_{log}, K	maxT_C, K
BaH_6 (100)	0.77	878	38 [43]
LaH_{10} (210)	3.41	848	286 [22]
LaH_{10} (170)	–	–	250–260 [6,7]
HfH_2 (260)	0.87	–	13 [59]
HfH_{10} (250)	2.77	677	234 [55]
TaH_6 (300)	1.56	1151	136 [60]
New predicted compounds			
HfH_{14} (300)	0.93	1138	76
BaH_{12} (135)	2.64	927	214

The data from our evolutionary searches for Hf-H phases at different pressures are shown in Supporting Information Fig. S6. The obtained data show the existence of novel higher hafnium hydrides, *Amm2*-Hf_3H_{13} at 100 GPa with T_C = 43 K, and *C2/m*-HfH_{14} at 300 GPa with T_C = 76 K (Supporting Information Fig. S25). Remarkably, more recent research of Xie et al. [55] points to possible stability of $P6_3/mmc$-HfH_{10} with $\lambda = 2.77$ and T_C = 234 K at 250 GPa in accordance with proposed the maxT_C(N_d) dependence.

The results for *P4/mmm*-BaH_6 obtained in Ref. [43] show quite low T_C. According to the logic of this work, Ba-H system should contain hydrides with a higher T_C, such as BaH_{10} and BaH_{12}, as it is for the other alkaline-earth elements. Barium is the closest neighbor of the La-H system with the record high-T_C superconductor LaH_{10} [6,7], and it is reasonable to expect remarkable superconducting properties in barium hydrides. Indeed, preliminary experimental results [62] confirm the existence of a pseudo-cubic BaH_{12}, stable at pressures over 80GPa, with the predicted by our neural network maxT_C of 214 K (Fig. 4).

The stability of the *Fdd2*-TaH_6 phase (maxT_C = 136 K at 300 GPa) is also questionable. Zhuang et al. [60] performed calculations using ELocR code and a limited integer set of possible TaH_n compositions with n = 1–6. However, such a high pressure may cause *Fdd2*-TaH_6 to be expelled from the convex hull by other compounds. Actually the comparison with the neighboring systems V-H, Nb-H, and Hf-H shows that maxT_C(Ta-H) should lie in the range of 40 to 90 K. The recent experimental investigation of the Ta-H system did not show the presence of any higher tantalum hydrides, only $TaH_{\sim 3}$ and $TaH_{\sim 2}$ were found [61]. Recalculation of Ta-H system done by Li et al. [63] indicated that $P2_1/c$-TaH_5 with maxT_C 23 K (100 GPa) is the most stable Ta-polyhydride at moderate pressures.

3.4. Lanthanoids and actinoids

Higher hydrides of lanthanoids are of particular interest because the theoretically predicted LaH_{10} [22] is the highest-T_C superconductor confirmed experimentally [6,7]. Peng et al. [64] conducted a theoretical study of lanthanoid hydrides, looking in particular at the formation of clathrate cages composed of the H atoms. Assuming REH_n (n = 8–10) to be thermodynamically stable, T_C was estimated at ~56 K at 100–200 GPa for Ce and Pr [64]. Our calculations for $P6_3mc$-CeH_6, found T_C not exceeding 51 K. Recent theoretical predictions and experimental synthesis of CeH_9 by Salke et al. [65] show that $P6_3/mmc$-CeH_9 should have $\lambda = 2.30$, ω_{log} = 740 K, and T_C = 117 K at 200 GPa (using Allen-Dynes formula and assuming μ^* = 0.1 as usual). Preliminary measurements of superconducting properties in the Ce-H system confirmed the predicted T_C of CeH_9 to be 100–110 K in the pressure range of 110 to 140 GPa [62], while for PrH_9 [14], NdH_9 [15] and UH_7 [62] - no superconducting transitions above 10 K were found.

To gain a more precise insight into the superconductivity of lanthanoid hydrides, we performed variable-composition evolutionary searches for thermodynamically stable compounds and crystal structures in almost all these systems. The obtained data are presented in Supporting Information Tables S1, S3-5.

According to the calculated results, most of the lanthanoid hydrides have a low EPC parameter (λ) and are weak superconductors (even neglecting magnetism). The critical temperatures display a monotonic decrease as the *f*-shell is getting filled, with the maximum T_C displayed in lanthanum and cerium hydrides (Fig. 5). Moving from the light to heavy lanthanoids, we observe vanishing of superconductivity for hydrides of metals with half-filled *d*- and *f*-shells (Mn – d^5, Re – d^5, Eu – f^7, Am – f^7), and then gradually increase in a "secondary wave" of superconductivity upon further filling of the *d*- and *f*-shells. We think this is because of the known stability of half-filled *d*- and *f*-shells, making

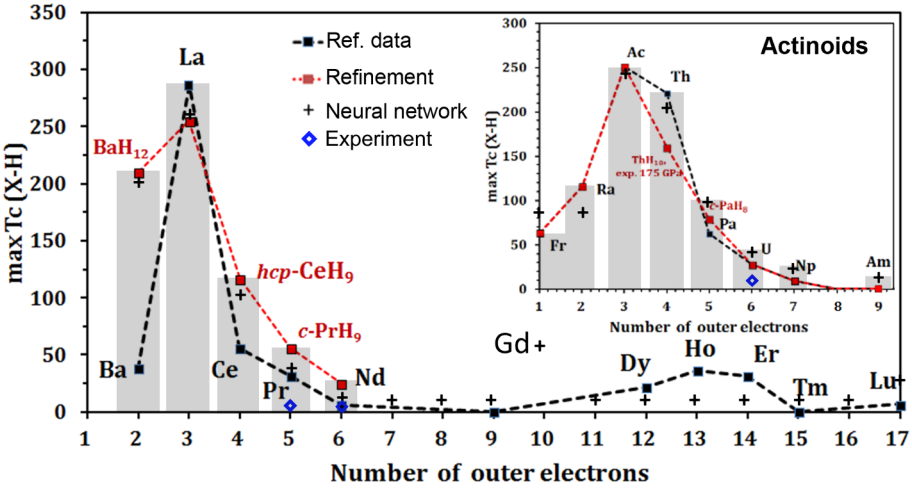

Fig. 5. Maximum critical temperature (maxT_C) in lanthanoid and actinoid hydrides as a function of the number of outer electrons in the metal atom. One can see predicted "secondary wave" of superconductivity in hydrides of heavy lanthanoids. Current experimental data of T_C for ThH_{10}, PrH_9, NdH_9 and UH_7 (blue diamonds) were taken from Refs. [11–13,62]. All ab initio calculations shown here were non-magnetic. (For interpretation of the references to color in this figure legend, the reader is referred to the web version of this article.)

these atoms exactly opposite of the electronically labile atoms amenable to high-T_C superconductivity.

The significant difference between the structures of hydrides of *d*- and *f*-elements is shown in Supporting Information Tables S4 and S5. The "pure" *d*-elements (Y, La, Ac, and Th) tend to form higher hydrides with cubic crystal structure, such as XH_{10}, with XH_{32} clathrate cages. Adding two or more *f*-electrons leads to changes in the crystal structure: the cubic XH_8 motif becomes predominant for the hydrides at 150 GPa. As long as the *f*-shell is filled sequentially within a certain range, the situation does not change much, as illustrated by the series of stable polyhydrides: $Fm\bar{3}m$-PaH_8, $Fm\bar{3}m$-UH_8, $Fm\bar{3}m$-NpH_8, and $Fm\bar{3}m$-AmH_8.

The new effect - the formation of a unique layered structure with hydrogen nonagons (9-cornered polygons) - was observed in erbium hydride $P\bar{6}m2$-ErH_{15} (Supporting Information Table S5). The closest analog with a similar crystal structure is $P\bar{6}m2$-AcH_{16}.[24] The hydrogen nonagons have not been observed in any other superhydrides considered above. Lutetium, despite having one *d*-electron and a completely filled *f*-shell, is not an analog of the d^1-elements Sc-Y-La-Ac because contribution of f-orbitals to the electronic structure of Lu hydrides is still significant. . LuH_{13} contains molecular fragments and is a semiconductor like many other hydrides of heavy lanthanoids and actinoids.

An increase in the number of *f*-electrons in actinoid hydrides also has an adverse effect on their superconductivity. We investigated the Pa-H, Np-H, Am-H, and Cm-H systems in addition to the already studied Ac-H [24], Th-H [23], and U-H [10] systems (Table 6) to confirm that maxT_C decreases as the number of *f*-electrons grows. The dependence of maxT_C on the number of outer electrons is shown in the inset in Fig. 5. Pr ($4f^3 6s^2$) and Pa ($5f^2 6d^1 7s^2$) have the same total number of *d*- and *f*-electrons, but T_C(Pa-H) > T_C(Pr-H) [66], because more localized *f*-electrons suppress superconductivity more than *d*-electrons (see details in the statistics section of Supporting Information).

The hydrides of actinoids allow us to suggest that the critical temperature decreases as the total number of *d*- and *f*-electrons grows. The highest critical temperature among the hydrides of actinoids, 251 K, belongs to the Ac-H system. It starts the sequence of critical temperatures decreasing monotonically in the Ac-Th-Pa-U-Np-Am series as the total number of *d*- and *f*-electrons increases. The data obtained for the newly predicted metal hydrides are summarized in Table 6.

All lanthanoids were combined in a single group because of their similar physical and chemical properties (electronic structure, atomic radii, electronegativity, etc.). For light lanthanoids, the crystal structures and compositions of pressure-stabilized hydrides are also similar (Fig. 6). The unexpected result is the extremely strong dependence of the superconducting critical temperature on the number of $d + f$ electrons. Despite the same structure and seemingly the same stabilization pressure of the metallic hydrogen sublattice of $Fm\bar{3}m$-PrH_8, $Fm\bar{3}m$-NdH_8, and $Fm\bar{3}m$-TmH_8, they have completely different λ, T_C and N_F (Supporting Information Tables S7 and S8) even in non-magnetic calculations. This clearly shows the crucial importance of the lanthanoid atom in superconductivity – i.e. that lanthanoid hydrides should not be considered as analogs of metallic hydrogen.

Physical meaning of the maxT_C(N_{d+f}) dependence can be explained starting from the idea of electron doping of hydrogen sublattice. As the number of d- and f-electrons of the lanthanoid atom increases, charge transfer to hydrogen (as measured by Bader charges) decreases (see [17]), and decrease of the number of electrons in the H-sublattice contributes to weakening superconductivity. Note that so far we referred to non-magnetic calculations (and indeed, most hydrides considered so far are non-magnetic). If magnetic ordering appears (as, e.g., in neodymium hydrides [15]), superconductivity may be completely suppressed. This will only strengthen our conclusions and the dependence of maxTc on the nature of the metal atom.

Using the data from Refs. [15,18,21,22,37,38,62–66,68–73] for the La-H, Y-H, Ca-H, K-H, Ac-H, Th-H, and Sc-H systems, the dependence of maxT_C on the number of hydrogen atoms *n* in the XH_n compounds was determined (Fig. 6a). The highest maxT_C values were achieved in compositions with n = 6…12 and particularly n = 10 (Y, La, Th, Ac). Further growth of n (>12) often leads to the formation of molecular hydrides with low T_C. As molecular hydrogen transforms to monoatomic at ≥ 500 GPa, such stoichiometries can also be very high-T_C superconductors at pressures above molecular dissociation.

The Ashby plot of maxT_C versus pressure (Fig. 6b) helps to identify the superconducting metal hydrides with the highest T_C and lowest stabilization pressure. From these two criteria, the best superconductors

Table 6
Parameters of superconductivity of the newly predicted metal hydrides. The critical temperatures were calculated using the Allen-Dynes formula [67] with $\mu^* = 0.1$.

Phases	*P*, GPa	λ	ω_{log}, K	T_C, K	$N(E_F)$, $eV^{-1}f.u.^{-1}$	$\mu_0 Hc$, T	Δ, meV
C2/m-TiH_{14}	200	0.81	1063	54	0.87	12	8.8
Immm-KH_{10}	150	1.34	1301	148	0.40	27	27.9
C2/m-CaH_{12}	150	2.16	1074	206	0.62	55.7	45
$P2_1/c$-ZrH_{16}	200	1.19	852	88	0.75	41.7	16.2
Amm2-Hf_3H_{13}	100	1.10	497	43	0.33	6.4	7.6
C2/m-HfH_{14}	300	0.93	1138	76	0.37	11.3	12.8
P4/nmm-FrH_7*	100	1.08	745	64	0.15	6.4	11.3
C2/m-RaH_{12}*	200	1.36	998	116	0.51	22	23
I4/mmm-BaH_{12}	135	2.66	927	214	0.30	43	49

* See Supporting Information for details.

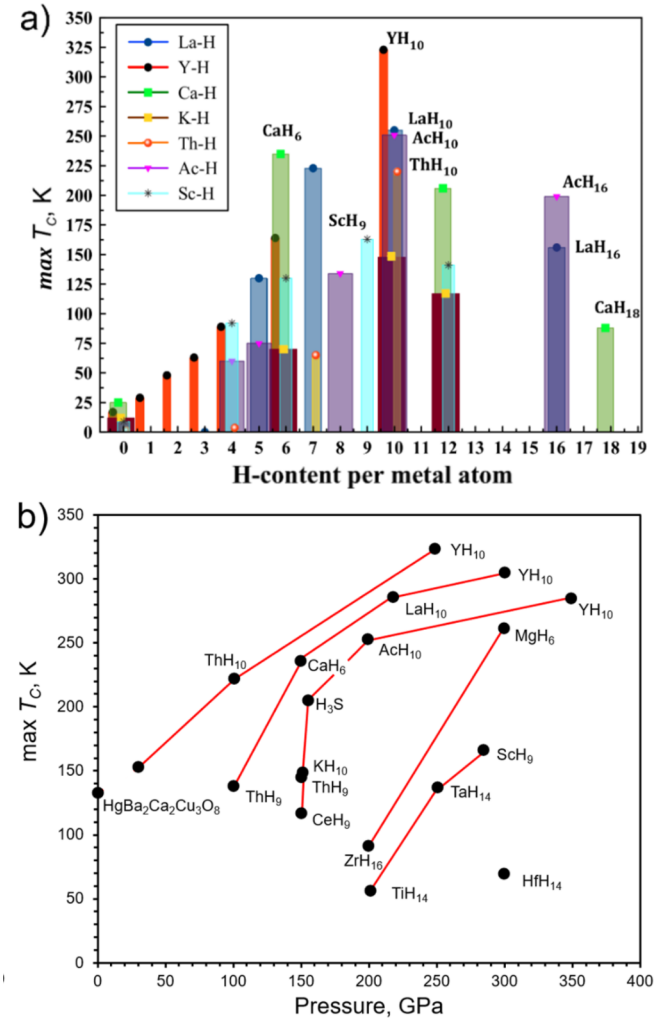

Fig. 6. (a) Maximum T_C for a given hydrogen content per metal atom in the XH_n hydrides, calculated using the Allen-Dynes formula. (b) Ashby plot of the maximum T_C versus pressure for the best-known calculated metal hydrides.

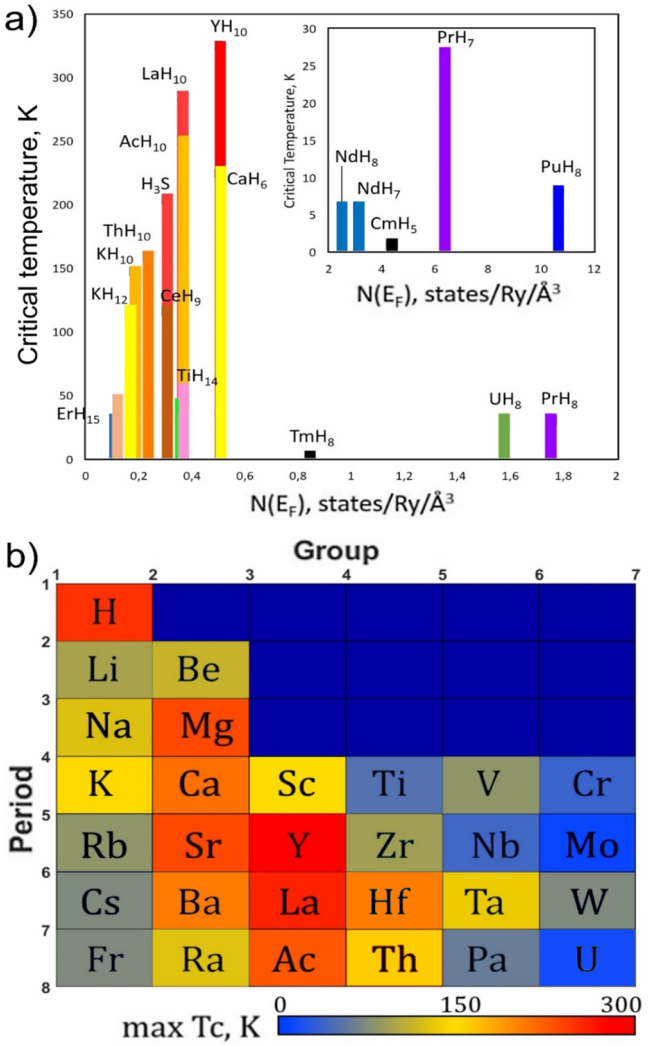

Fig. 7. (a) Maximum predicted T_C versus the electronic density of states at Fermi level for the studied hydrides. (b) The distribution of maxT_C of metal hydrides in the left part of Mendeleev's.

are $HgBa_2Ca_2Cu_3O_8$ [74], ThH_{10}, CaH_6, LaH_{10} and YH_{10}. The expected critical temperature increases with pressure, probably reaches the maximum at 200–250 GPa, and then decreases. Seemingly, the pressure range from 100 to 250 GPa is required to achieve $T_C > 200$ K in metal hydrides.

The highest T_C values usually correspond to transfer of ~0.3 electron per H-atom [64]. For example, it is 0.33e in CaH_6 and MgH_6, 0.30e in YH_{10} and LaH_{10}, 0.40e in ThH_{10}. These additional electrons weaken H-H bonds and this amount of electrons is sufficient for breaking H_2 molecules while keeping weak H-H bonds (recall that any electrons added to the H_2 molecule occupy the antibonding orbital; also recall that molecular H_2-groups in polyhydrides are unfavorable for high-Tc superconductivity). Looking at the highest-Tc superconductors, which are in the YH_{10}-LaH_{10}-AcH_{10} series, the electronic density of states at the Fermi level ($N(E_F)$) is 10–12 states/Ry/cell, or 0.3–0.5 states/Ry/Å^3, or ~1 state/Ry/H-atom at 200–250 GPa. A deviation from this value results in a sharp decrease in the superconducting properties (Fig. 7a and Supporting Information Table S7).

The geometric profile of the distribution of superconducting properties of metal hydrides in a part of Mendeleev's Table is shown in Fig. 7b. The region of highest Tc values runs along the "lability belt" between 2nd and 3rd groups, and is slanted towards 4th group for heavier elements.

The distribution of the EPC coefficients λ and logarithmic average frequencies ω_{log} over Mendeleev's Periodic Table, corresponding to maxT_C of the studied hydrides, is shown in Fig. 8. While the highest value of ω_{log} are predictably concentrated in the area of light elements, distribution of λ coincides with that of maxT_C: the maximum values belong to the hydrides from the d^0 and d^1 belts (Fig. 8a). This is not surprising because the record superconductivity is almost always associated with anomalously high λ values. The distribution of ω_{log} (Fig. 8b) reaches the maximum for hydrides of light elements (H-Be-Li-Mg). It is well known that light elements tend to undergo the same transitions as heavier elements, but at higher pressures (here, >200-300 GPa).

According to the obtained data and proposed rules, the most pronounced superconducting properties could be expected for hydrides of the elements located at the boundary between blocks of the Periodic Table (*s-p, s-d, p-d, d-f*).

4. Conclusions

Detailed analysis of both obtained and available reference data enabled us to propose the rules rationalizing superconductivity of metal hydrides over Mendeleev's Table. Using our rule of electronic lability, we questioned and successfully corrected previous results on K-H, Zr-H, Hf-H and Ti-H systems. New hydrides were also predicted in Mg-H, Sr-

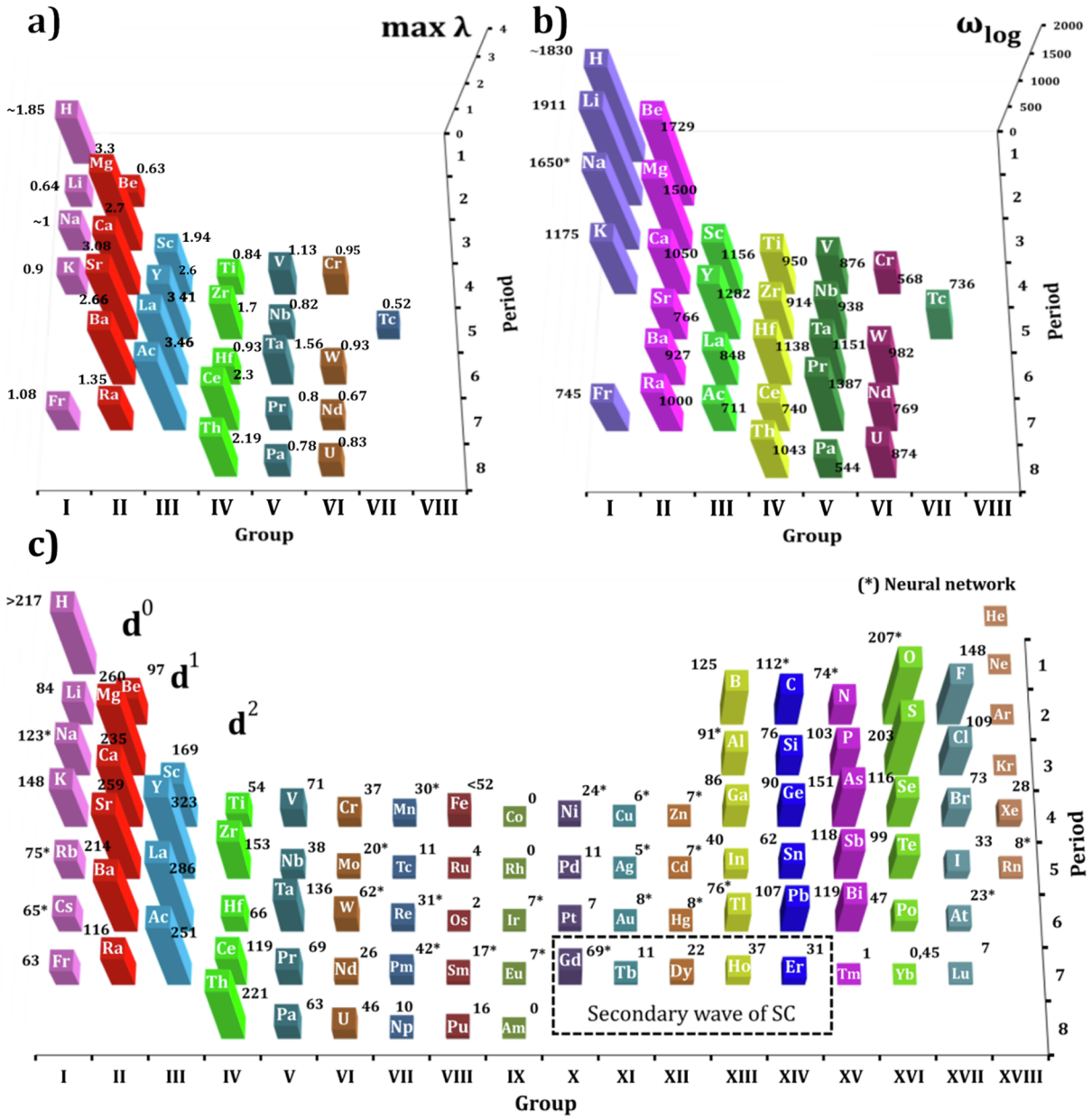

Fig. 8. Distribution of (a) the EPC coefficient λ and (b) logarithmic average frequency ω_{log} corresponding to the maxT_C points over Mendeleev's Table. The data for hydrogen were taken from Refs. [75,76]; the data for Na-H were estimated using our neural network. .(c) Mendeleev's Table with already studied binary hydrides. The maximum values of Tc were calculated using ab initio or were predicted by the developed neural network (marked by *).

H, Ba-H, Cs-H and Rb-H systems. Our main conclusions are:

- Most of the high-temperature superconducting metal hydrides are concentrated in the "lability belt" of Mendeleev's Table. The metals forming the high-T_C hydrides are: Sc-Y-La-Ac (d^1 belt), Mg-Ca-Sr-Ba-Ra (d^0 belt), and Th (s^2d^2). These elements are electronically labile, i.e. their orbital populations should be sensitive to atomic environment, giving rise to strong electron-phonon coupling;
- Maximum values of T_C are achieved when the number of electrons transferred from metal atoms is ~0.3*e* per hydrogen atom. The electronic density of states at the Fermi level $N(E_F)$ of the highest-Tc superconducting hydrides is ~1 state/Ry/H-atom.
- The superconducting properties of hydrides greatly diminish as the number of *d*- and *f*-electrons increases. In particular, the critical temperatures of lanthanoid and actinoid hydrides decrease almost monotonically with increasing number of *f*-electrons.
- Optimal hydrogen content in superconductors corresponds to $XH_{10\pm2}$ composition which can be formed at pressures of about 150–250 GPa. If the composition or/and the level of electron doping deviate from the optimal values, the superconductivity parameters decrease.
- The pressure required for the stabilization of hydrides decreases going down the Periodic Table. For actinoids, the pressure of 50 GPa is enough to stabilize superconducting polyhydrides, like UH_7 and PaH_8.

Credit authorship contribution statement

D.V.S. conceived this project and performed calculations of superconductivity. I.A.K. for USPEX. searches I.A.S. developed the neural network. A.G.K. calculated physical properties of metal hydrides and prepared manuscript. A.G.K., D.V.S. and A.R.O. wrote and revised the paper and developed its main ideas.

Declaration of Competing Interest

The authors declare that they have no known competing financial interests or personal relationships that could have appeared to influence the work reported in this paper.

Acknowledgments

A.R.O. is grateful to the Russian Science Foundation (№ 19-72-30043). The calculations were performed on Rurik supercomputer at the MIPT. The authors thank Dr. Mahdi Davari Esfahani for the study of stable phases in the Cm-H system. A.G.K. thanks the Foundation for Assistance to Small Innovative Enterprises (FASIE) for the financial support within the UMNIK grant № 13408GU/2018 and Russian Foundation for Basic Research (RFBR) project № 19-03-00100.

Data availability

The authors declare that all other data supporting the findings of this study are available within the paper and its supplementary information files

Appendix A. Supplementary material

The crystal data, convex hulls, Eliashberg functions, forecast list, and statistical data for the studied metal polyhydrides are included in Supporting Information. Supplementary data to this article can be found online at https://doi.org/10.1016/j.cossms.2020.100808.

References

[1] A.P. Drozdov, M.I. Eremets, I.A. Troyan, V. Ksenofontov, S.I. Shylin, Conventional superconductivity at 203 Kelvin at high pressures in the sulfur hydride system, Nature 525 (7567) (2015) 73–76, https://doi.org/10.1038/nature14964.
[2] D. Duan, Y. Liu, Y. Ma, Z. Shao, B. Liu, T. Cui, Structure and superconductivity of hydrides at high pressures, Natl. Sci. Rev. 4 (1) (2017) 121–135, https://doi.org/10.1093/nsr/nww029.
[3] A.K. Mishra, M. Somayazulu, M. Ahart, A. Karandikar, R.J. Hemley, V.V. Struzhkin, Novel synthesis route and observation of superconductivity in the Se-H system at extreme conditions, Bulletin of the American Physical Society, (2018).
[4] P.P. Kong, A.P. Drozdov, E. Eroke, M.I. Eremets, Pressure-induced superconductivity above 79 K in Si2H6, Book of abstracts of AIRAPT 26 joint with ACHPR 8 & CHPC 19; Biijing, China, 2017, p. 347.
[5] Z.M. Geballe, H. Liu, A.K. Mishra, M. Ahart, M. Somayazulu, Y. Meng, M. Baldini, R.J. Hemley, Synthesis and stability of lanthanum superhydrides, Angew. Chem. Int. Ed. 57 (3) (2017) 688–692, https://doi.org/10.1002/anie.201709970.
[6] A.P. Drozdov, P.P. Kong, V.S. Minkov, S.P. Besedin, M.A. Kuzovnikov, S. Mozaffari, L. Balicas, F.F. Balakirev, D.E. Graf, V.B. Prakapenka, et al., Superconductivity at 250 K in lanthanum hydride under high pressures, Nature 569 (7757) (2019) 528, https://doi.org/10.1038/s41586-019-1201-8.
[7] M. Somayazulu, M. Ahart, A.K. Mishra, Z.M. Geballe, M. Baldini, Y. Meng, V.V. Struzhkin, R.J. Hemley, Evidence for superconductivity above 260 K in lanthanum superhydride at megabar pressures, Phys. Rev. Lett. 122 (2) (2019) 027001, https://doi.org/10.1103/PhysRevLett.122.027001.
[8] C.M. Pépin, G. Geneste, A. Dewaele, M. Mezouar, P. Loubeyre, Synthesis of FeH_5: A layered structure with atomic hydrogen slabs, Science 357 (6349) (2017) 382–385, https://doi.org/10.1126/science.aan0961.
[9] A. Majumdar, J.S. Tse, M. Wu, Y. Yao, Superconductivity in FeH_5, Phys. Rev. B 96 (20) (2017) 201107, https://doi.org/10.1103/PhysRevB.96.201107.
[10] I.A. Kruglov, A.G. Kvashnin, A.F. Goncharov, A.R. Oganov, S.S. Lobanov, N. Holtgrewe, Sh Jiang, V.B. Prakapenka, E. Greenberg, A.V. Yanilkin, Uranium polyhydrides at moderate pressures: prediction, synthesis, and expected superconductivity, Sci. Adv. 4 (10) (2018), https://doi.org/10.1126/sciadv.aat9776 eaat9776.
[11] X. Li, X. Huang, D. Duan, C.J. Pickard, D. Zhou, H. Xie, Q. Zhuang, Y. Huang, Q. Zhou, B. Liu, et al., Polyhydride CeH_9 with an atomic-like hydrogen clathrate structure, Nat. Commun. 10 (1) (2019) 3461, https://doi.org/10.1038/s41467-019-11330-6.
[12] N.P. Salke, M.M.D. Esfahani, Y. Zhang, I.A. Kruglov, J. Zhou, Y. Wang, E. Greenberg, V.B. Prakapenka, J. Liu, A.R. Oganov, et al., Synthesis of clathrate cerium superhydride CeH_9 at 80–100 GPa with atomic hydrogen sublattice, Nat. Commun. 10 (1) (2019) 4453, https://doi.org/10.1038/s41467-019-12326-y.
[13] D.V. Semenok, A.G. Kvashnin, A.G. Ivanova, V. Svitlyk, V.Y. Fominski, A.V. Sadakov, O.A. Sobolevskiy, V.M. Pudalov, I.A. Troyan, A.R. Oganov, Superconductivity at 161 K in thorium hydride ThH_{10}: synthesis and properties, Mater. Today (2019), https://doi.org/10.1016/j.mattod.2019.10.005.
[14] D. Zhou, D. Semenok, D. Duan, H. Xie, X. Huang, W. Chen, X. Li, B. Liu, A.R. Oganov, T. Cui, Superconducting praseodymium superhydrides, Sci. Adv. (2020), https://doi.org/10.1126/sciadv.aax6849.
[15] D. Zhou, D.V. Semenok, H. Xie, X. Huang, D. Duan, A. Aperis, P.M. Oppeneer, M. Galasso, A.I. Kartsev, A.G. Kvashnin, et al., High-pressure synthesis of magnetic neodymium polyhydrides, J. Am. Chem. Soc. (2020), https://doi.org/10.1021/jacs.9b10439.
[16] Y. Xe, Q. Li, A.R. Oganov, H. Wang, superconductivity of lithium-doped hydrogen under high pressure, Acta Cryst. C 70 (2014) 104–111.
[17] H. Wang, J.S. Tse, K. Tanaka, T. Iitaka, Y. Ma, Superconductive sodalite-like clathrate calcium hydride at high pressures, Proc. Natl. Acad. Sci. 109 (17) (2012) 6463–6466, https://doi.org/10.1073/pnas.1118168109.
[18] K. Tanaka, J.S. Tse, H. Liu, Electron-phonon coupling mechanisms for hydrogen-rich metals at high pressure, Phys. Rev. B 96 (10) (2017) 100502, https://doi.org/10.1103/PhysRevB.96.100502.
[19] G. Gao, R. Hoffmann, N.W. Ashcroft, H. Liu, A. Bergara, Y. Ma, Theoretical study of the ground-state structures and properties of niobium hydrides under pressure, Phys. Rev. B 88 (18) (2013) 184104, https://doi.org/10.1103/PhysRevB.88.184104.
[20] K. Abe, Hydrogen-rich scandium compounds at high pressures, Phys. Rev. B 96 (14) (2017) 144108, https://doi.org/10.1103/PhysRevB.96.144108.
[21] X. Li, F. Peng, Superconductivity of pressure-stabilized vanadium hydrides, Inorg. Chem. 56 (22) (2017) 13759–13765, https://doi.org/10.1021/acs.inorgchem.7b01686.
[22] H. Liu, I.I. Naumov, R. Hoffmann, N.W. Ashcroft, R.J. Hemley, Potential high-Tc superconducting lanthanum and yttrium hydrides at high pressure, Proc. Natl. Acad. Sci. 114 (2017) 6990–6995, https://doi.org/10.1073/pnas.1704505114.
[23] A.G. Kvashnin, D.V. Semenok, I.A. Kruglov, I.A. Wrona, A.R. Oganov, High-temperature superconductivity in Th-H system at pressure conditions, ACS Appl. Mater. Interfaces 10 (50) (2018) 43809–43816.
[24] D.V. Semenok, A.G. Kvashnin, I.A. Kruglov, A.R. Oganov, Actinium hydrides AcH_{10}, AcH_{12}, and AcH_{16} as high-temperature conventional superconductors, J. Phys. Chem. Lett. 9 (8) (2018) 1920–1926, https://doi.org/10.1021/acs.jpclett.8b00615.
[25] A.R. Oganov, C.W. Glass, Crystal structure prediction using ab initio evolutionary techniques: principles and applications, J. Chem. Phys. 124 (2006) 244704, https://doi.org/10.1063/1.2210932.
[26] A.R. Oganov, A.O. Lyakhov, M. Valle, How evolutionary crystal structure prediction works—and why, Acc. Chem. Res. 44 (2011) 227–237, https://doi.org/10.1021/ar1001318.
[27] A.O. Lyakhov, A.R. Oganov, H.T. Stokes, Q. Zhu, New developments in evolutionary structure prediction algorithm USPEX, Comput. Phys. Commun. 184 (2013) 1172–1182, https://doi.org/10.1016/j.cpc.2012.12.009.
[28] P.V. Bushlanov, V.A. Blatov, A.R. Oganov, Topology-based crystal structure generator, Comput. Phys. Commun. 236 (2019) 1–7, https://doi.org/10.1016/j.cpc.2018.09.016.
[29] P. Hohenberg, W. Kohn, Inhomogeneous electron gas, Phys. Rev. 136 (3B) (1964) B864–B871.
[30] W. Kohn, L.J. Sham, Self-consistent equations including exchange and correlation effects, Phys. Rev. 140 (4) (1965) A1133–A1138.
[31] J.P. Perdew, K. Burke, M. Ernzerhof, Generalized gradient approximation made simple, Phys. Rev. Lett. 77 (18) (1996) 3865–3868.
[32] P.E. Blöchl, Projector augmented-wave method, Phys. Rev. B 50 (24) (1994) 17953–17979, https://doi.org/10.1103/PhysRevB.50.17953.
[33] G. Kresse, D. Joubert, From ultrasoft pseudopotentials to the projector augmented-wave method, Phys. Rev. B 59 (3) (1999) 1758–1775, https://doi.org/10.1103/PhysRevB.59.1758.
[34] G. Kresse, J. Furthmüller, Efficient iterative schemes for ab initio total-energy calculations using a plane-wave basis set, Phys. Rev. B 54 (1996) 11169–11186, https://doi.org/10.1103/PhysRevB.54.11169.
[35] G. Kresse, J. Hafner, Ab initio molecular dynamics for liquid metals, Phys. Rev. B 47 (1993) 558–561, https://doi.org/10.1103/PhysRevB.47.558.
[36] G. Kresse, J. Hafner, Ab initio molecular-dynamics simulation of the liquid-metal amorphous-semiconductor transition in germanium, Phys. Rev. B 49 (1994) 14251–14269, https://doi.org/10.1103/PhysRevB.49.14251.
[37] S. Baroni, S. de Gironcoli, A. Dal Corso, P. Giannozzi, Phonons and related crystal properties from density-functional perturbation theory, Rev. Mod. Phys. 73 (2) (2001) 515–562.
[38] P. Giannozzi, S. Baroni, N. Bonini, M. Calandra, R. Car, C. Cavazzoni, D. Ceresoli, G.L. Chiarotti, M. Cococcioni, I. Dabo, et al., QUANTUM ESPRESSO: A modular and open-source software project for quantum simulations of materials, J. Phys. Condens. Matter 21 (2009) 395502, https://doi.org/10.1088/0953-8984/21/39/395502.
[39] D. Zhou, X. Jin, X. Meng, G. Bao, Y. Ma, B. Liu, T. Cui, Ab initio study revealing a layered structure in hydrogen-rich KH_6 under high pressure, Phys. Rev. B 86 (1) (2012) 14118, https://doi.org/10.1103/PhysRevB.86.014118.
[40] X. Ye, N. Zarifi, E. Zurek, R. Hoffmann, N.W. Ashcroft, High hydrides of scandium under pressure: potential superconductors, J. Phys. Chem. C 122 (11) (2018) 6298–6309, https://doi.org/10.1021/acs.jpcc.7b12124.
[41] K.V. Shanavas, L. Lindsay, D.S. Parker, Electronic structure and electron-phonon coupling in TiH_2, Sci. Rep. 6 (2016) 28102, https://doi.org/10.1038/srep28102.
[42] S. Yu, X. Jia, G. Frapper, D. Li, A.R. Oganov, Q. Zeng, L. Zhang, Pressure-driven formation and stabilization of superconductive chromium hydrides, Sci. Rep. 5 (2015) 17764, https://doi.org/10.1038/srep17764.
[43] J. Hooper, B. Altintas, A. Shamp, E. Zurek, Polyhydrides of the alkaline earth metals: A look at the extremes under pressure, J. Phys. Chem. C 117 (6) (2013) 2982–2992, https://doi.org/10.1021/jp311571n.

[44] J. Hooper, E. Zurek, High pressure potassium polyhydrides: A chemical perspective, J. Phys. Chem. C 116 (24) (2012) 13322–13328, https://doi.org/10.1021/jp303024h.

[45] A.K. Mishra, T.S. Muramatsu, H. Liu, Z.M. Geballe, M. Somayazulu, M. Ahart, M. Baldini, Y. Meng, E. Zurek, R.J. Hemley, New calcium hydrides with mixed atomic and molecular hydrogen, J. Phys. Chem. C 122 (34) (2018) 19370–19378, https://doi.org/10.1021/acs.jpcc.8b05030.

[46] Z. Shao, D. Duan, Y. Ma, H. Yu, H. Song, H. Xie, D. Li, F. Tian, B. Liu, T. Cui, Unique phase diagram and superconductivity of calcium hydrides at high pressures, Inorg. Chem. 58 (4) (2019) 2558–2564, https://doi.org/10.1021/acs.inorgchem.8b03165.

[47] J. Zhang, J.M. McMahon, A.R. Oganov, X. Li, X. Dong, H. Dong, S. Wang, High-Temperature Superconductivity in the Ti–H System at High Pressures, ArXiv191109293 Cond-Mat, 2019.

[48] X. Li, H. Liu, F. Peng, Crystal structures and superconductivity of technetium hydrides under pressure, Phys. Chem. Chem. Phys. 18 (41) (2016) 28791–28796, https://doi.org/10.1039/C6CP05702K.

[49] X.-F. Li, Z.-Y. Hu, B. Huang, Phase diagram and superconductivity of compressed zirconium hydrides, Phys. Chem. Chem. Phys. 19 (5) (2017) 3538–3543, https://doi.org/10.1039/C6CP08036G.

[50] J. Hooper, E. Zurek, rubidium polyhydrides under pressure: emergence of the linear H_3- species - hooper - 2012 - chemistry 8211; A European journal - wiley online library, Chem. Eur. J. 18 (2012) 5013–5021.

[51] M.J. Hutcheon, A.M. Shipley, R.J. Needs, Predicting Novel Superconducting Hydrides Using Machine Learning Approaches, ArXiv200109852 Cond-Mat, 2020.

[52] G. Wu, X. Huang, H. Xie, X. Li, M. Liu, Y. Liang, Y. Huang, D. Duan, F. Li, B. Liu, et al., Unexpected calcium polyhydride CaH_4: A possible route to dissociation of hydrogen molecules, J. Chem. Phys. 150 (4) (2019) 44507, https://doi.org/10.1063/1.5053650.

[53] K. Abe, High-pressure properties of dense metallic zirconium hydrides studied by ab initio calculations, Phys. Rev. B 98 (13) (2018) 134103, https://doi.org/10.1103/PhysRevB.98.134103.

[54] H. Xie, W. Zhang, D. Duan, X. Huang, Y. Huang, H. Song, X. Feng, Y. Yao, C.J. Pickard, T. Cui, Superconducting zirconium polyhydrides at moderate pressures, J. Phys. Chem. Lett. 11 (3) (2020) 646–651, https://doi.org/10.1021/acs.jpclett.9b03632.

[55] H. Xie, Y. Yao, X. Feng, D. Duan, H. Song, Z. Zhang, S. Jiang, S.A.T. Redfern, V.Z. Kresin, C.J. Pickard, et al., Hydrogen "Penta-Graphene-like" Structure Stabilized via Hafnium: A High-Temperature Conventional Superconductor, ArXiv200104076 Cond-Mat, 2020.

[56] P.P. Kong, V.S. Minkov, M.A. Kuzovnikov, S.P. Besedin, A.P. Drozdov, S. Mozaffari, L. Balicas, F.F. Balakirev, V.B. Prakapenka, E. Greenberg, et al., Superconductivity up to 243 K in yttrium hydrides under high pressure, ArXiv190910482 Cond.-Mat. (2019).

[57] APS-APS March Meeting 2020 - Event - Superconductivity at 262 K in Yttrium Superhydride at High Pressures, in: Bulletin of the American Physical Society, American Physical Society, 2020.

[58] A. Shamp, J. Hooper, E. Zurek, Compressed cesium polyhydrides: Cs+ sublattices and H_3- three-connected nets - inorganic chemistry (ACS Publications), Inorg. Chem. 51 (17) (2012) 9333–9342.

[59] A.M. Duda, K.A. Szewczyk, M.W. Jarosik, K.M. Szcześniak, M.A. Sowińska, D. Szcześniak, Characterization of the superconducting state in hafnium hydride under high pressure, Phys. B Condens. Matter 536 (2018) 275–279, https://doi.org/10.1016/j.physb.2017.10.107.

[60] Q. Zhuang, X. Jin, T. Cui, Y. Ma, Q. Lv, Y. Li, H. Zhang, X. Meng, K. Bao, Pressure-stabilized superconductive ionic tantalum hydrides, Inorg. Chem. 56 (7) (2017) 3901–3908, https://doi.org/10.1021/acs.inorgchem.6b02822.

[61] J. Ying, X. Li, E. Greenberg, V.B. Prakapenka, H. Liu, V.V. Struzhkin, Synthesis and stability of tantalum hydride at high pressures, Phys. Rev. B 99 (22) (2019) 224504, https://doi.org/10.1103/PhysRevB.99.224504.

[62] Personal Information from Huang's Group, Jilin University.

[63] H. Li, X. Li, H. Wang, G. Liu, Y. Li, H. Liu, Superconducting TaH_5 at high pressure, New J. Phys. 21 (12) (2019) 123009, https://doi.org/10.1088/1367-2630/ab5a9a.

[64] F. Peng, Y. Sun, C.J. Pickard, R.J. Needs, Q. Wu, Y. Ma, Hydrogen clathrate structures in rare earth hydrides at high pressures: possible route to room-temperature superconductivity, Phys. Rev. Lett. 119 (2017) 107001–107007, https://doi.org/10.1103/PhysRevLett. 119.107001.

[65] N.P. Salke, M.M.D. Esfahani, Y. Zhang, I.A. Kruglov, J. Zhou, Y. Wang, E. Greenberg, V.B. Prakapenka, A.R. Oganov, J.-F. Lin, Synthesis of Clathrate Cerium Superhydride CeH9 at 80 GPa with Anomalously Short H-H Distance, arXiv:1805.02060, 2018, https://arxiv.org/ftp/arxiv/papers/1805/1805.02060.pdf.

[66] X. Xiao, D. Duan, H. Xie, Z. Shao, D. Li, F. Tian, H. Song, H. Yu, K. Bao, T. Cui, Structure and superconductivity of protactinium hydrides under high pressure, J. Phys. Condens. Matter 31 (31) (2019) 315403, https://doi.org/10.1088/1361-648X/ab1d03.

[67] P.B. Allen, R.C. Dynes, Transition temperature of strong-coupled superconductors reanalyzed, Phys. Rev. B 12 (3) (1975) 905–922, https://doi.org/10.1103/PhysRevB.12.905.

[68] V.V. Struzhkin, D.Y. Kim, E. Stavrou, T. Muramatsu, H. Mao, C.J. Pickard, R.J. Needs, V.B. Prakapenka, A.F. Goncharov, Synthesis of sodium polyhydrides at high pressures, Nat. Commun. 7 (2016) 12267, https://doi.org/10.1038/ncomms12267.

[69] I.A. Kruglov, D.V. Semenok, H. Song, R. Szczęśniak, I.A. Wrona, R. Akashi, M.M.D. Esfahani, D. Duan, T. Cui, A.G. Kvashnin, et al., Superconductivity of LaH_{10} and LaH_{16} Polyhydrides, Phys. Rev. B (2019) ASAP.

[70] J.J. Hamlin, V.G. Tissen, J.S. Schilling, Superconductivity at 17 K in yttrium metal under nearly hydrostatic pressures up to 89GPa, Phys. Rev. B 73 (9) (2006) 094522, https://doi.org/10.1103/PhysRevB.73.094522.

[71] T. Yabuuchi, T. Matsuoka, Y. Nakamoto, K. Shimizu, Superconductivity of Ca exceeding 25 K at megabar pressures, J. Phys. Soc. Jpn. 75 (8) (2006) 083703, https://doi.org/10.1143/JPSJ.75.083703.

[72] G. Profeta, C. Franchini, N.N. Lathiotakis, A. Floris, A. Sanna, M.A.L. Marques, M. Lüders, S. Massidda, E.K.U. Gross, A. Continenza, Superconductivity in lithium, potassium, and aluminum under extreme pressure: A first-principles study, Phys. Rev. Lett. 96 (4) (2006) 047003, https://doi.org/10.1103/PhysRevLett. 96.047003.

[73] L.W. Nixon, D.A. Papaconstantopoulos, M.J. Mehl, Calculations of the superconducting properties of scandium under high pressure, Phys. Rev. B 76 (13) (2007) 134512, https://doi.org/10.1103/PhysRevB.76.134512.

[74] A. Schilling, M. Cantoni, J.D. Guo, H.R. Ott, Superconductivity above 130 K in the Hg–Ba–Ca–Cu–O System, Nature 363 (6424) (1993) 56–58, https://doi.org/10.1038/363056a0.

[75] C.F. Richardson, N.W. Ashcroft, High temperature superconductivity in metallic hydrogen: electron-electron enhancements, Phys. Rev. Lett. 78 (1) (1997) 118–121, https://doi.org/10.1103/PhysRevLett. 78.118.

[76] T.W. Barbee, A. García, M.L. Cohen, First-principles prediction of high-temperature superconductivity in metallic hydrogen, Nature 340 (6232) (1989) 369, https://doi.org/10.1038/340369a0.